Status of VFCAL

M. Idzik, K. Swientek, Sz. Kulis, D. Przyborowski and L. Suszycki
AGH University of Science and Technology, Cracow, Poland

W. Daniluk , E. Kielar, J. Kotuła, K. Oliwa, B. Pawlik, W. Wierba and L. Zawiejski
Institute of Nuclear Physics PAN, Cracow, Poland

H. Abramowicz, R. Ingbir, S. Kananov, A. Levy, I. Sadeh and A. Stern
School of Physics and Astronomy, Tel Aviv University, Tel Aviv, Israel

H. Henschel, W. Lange, W. Lohmann, M. Ohlerich and S. Schuwalow
DESY, Zeuthen, Germany

December 10, 2008

Abstract

Within VFCAL in 2008 several milestones and deliverables have to be addressed: the development of sensor test facilities has to be completed, prototypes of the FE readout electronics have to be produced and a prototype of the laser alignment system has to be ready. For each of the deliverable a separate report or memo has been written. In this memo we briefly summarize the results.

1 Introduction

We face several challenges to develop the technologies for the two calorimeters planned in the very forward region of a future ILC detector [1]. The innermost calorimeter, BeamCal, has to withstand harsh radiation conditions and must be read out bunch-by-bunch. Hence radiation hard sensors must be found and fast FE ASICs have to be developed. At larger polar angles, LumiCal must be positioned precisely, and displacements with respect to the beam have to be controlled within a few 10 μm.
Sensors structured into pads need a readout electronics tolerating a large range of input capacitances, of a large dynamic range and being sufficiently fast.
Both calorimeters must be fine-grained and compact. Hence low-volume and low power dissipation FE ASICs are necessary.
The goal of the VFCAL project is to develop the infrastructure for tests of all subcomponents of these special calorimeters. This includes infrastructure to perform sensor studies in the laboratory and in test-beams, prototypes of sensors and FE electronics to be used for tests of components of the calorimeter in the beam, and a prototype of a high precision laser position monitoring system matching the precision requirements.

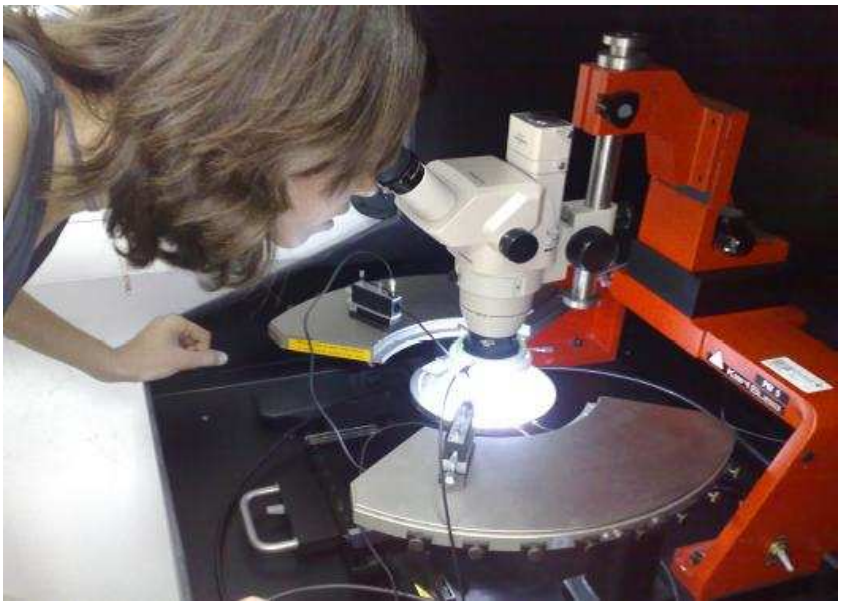

Figure 1: A student working at the probe-station in the sensor test laboratory at Tel Aviv University.

2 Sensor Test Facilities

For sensor tests the necessary laboratory infrastructure has been created in TAU and upgraded at DESY [2]. In addition, equipment for sensor irradiation and performance

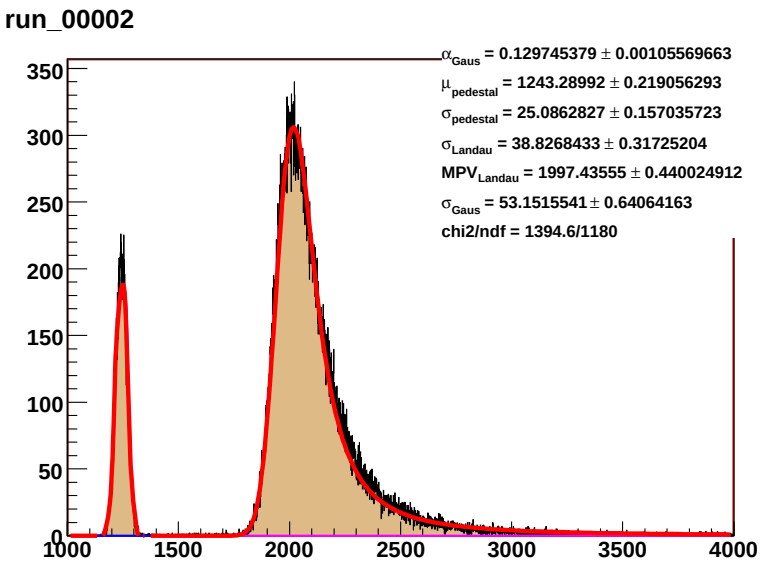

Figure 2: Signal spectrum of a single crystal diamond taken with the upgraded spectrometer setup.

studies has been designed, built and used in test-beams. Performance measurements have been done using this equipment together with the EUDET pixel telescope at DESY and at the S-DALINAC linear accelerator of the Technical University in Darmstadt.

2.1 Laboratory Infrastructure

At the Tel Aviv University a dedicated laboratory has been established to study silicon sensors [3] produced for the prototype of LumiCal. It comprises a manually controlled probe-station, shown in Figure 1, to measure currents and capacitances as a function of the bias voltage computer controlled. In 2009, this laboratory will be hosted in a new laboratory building together with a clean room and a set-up for spectroscopic measurements.

The existing silicon laboratory at DESY Zeuthen has been upgraded. New computer controlled high-voltage supplies are now installed and software for measurements on different sensor materials has been developed.

In addition, the set-up to measure spectra of radioactive sources has been revised. With new collimators and the use of two consecutive scintillator tiles as trigger counters we obtain very clean signal spectra from sensors as shown e.g. for a ^{90}Sr source in Figure 2.

A sub-micrometer x-y scan station has been prepared for semi-automated test of sensor structures with several pads and for the investigation of sensor performance across pad boundaries.

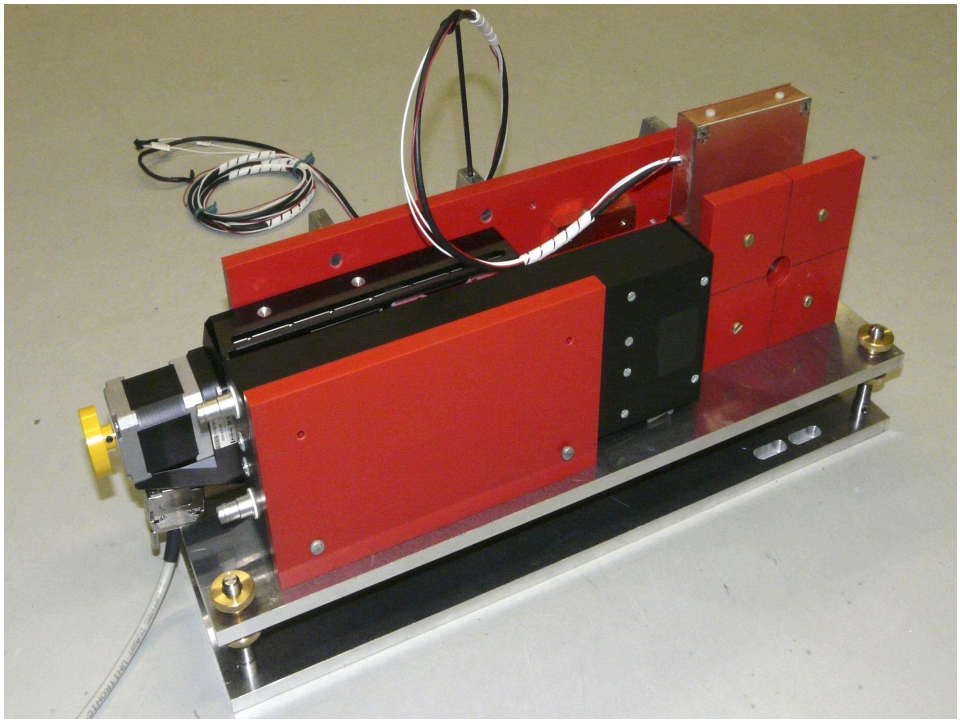

Figure 3: Test-beam setup for sensor irradiation in the DALINAC electron beam. On the left the computer controlled mover (with yellow wheel) is visible. The black box in the front (left) contains the scintillator trigger for spectroscopic measurements. At the right the setup for irradiation in a high intensity beam is located. The sensor is placed in the copper box (top right) between a collimator and a Faraday cup.

2.2 Test-beam Infrastructure

The test-beam equipment for sensor tests in low-energy electron beams has been completed and used several times at the S-DALINAC accelerator at the Technical University of Darmstadt. The set-up is shown in Figure 3 [1]. A beam of 10 MeV electrons is being used. A copper collimator (right, behind the red plastic wall) limits the cross section of the spread beam and measures the electron current dumped onto it. The sensor is positioned inside the copper box (top, with cables) between the collimator and a Faraday cup (rear), with bias voltage applied. The current caused by ionisation and the sensor temperature are measured. The Faraday cup collects all electrons traversing the sensor. Measuring the current, the dose rate can be determined. After a certain integrated dose is collected, the sensor box is moved remotely to the left, and the signals from electrons of a ^{90}Sr source are measured using the scintillator counters described above. Its peak position is determined, denoted hereafter as reference signal, and monitored as a function of the absorbed dose.

[1] In previous test-beam studies a simplified set-up described in Ref. [4] was used.

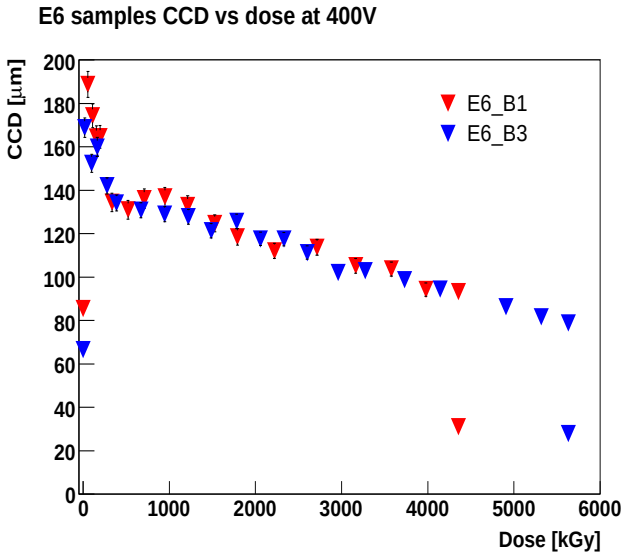

Figure 4: The signal size (expressed in charge collection distance, CCD) as a function of the absorbed dose, for two CVD diamond sensors.

Irradiation studies have been done with radiation hard silicon, GaAs and CVD diamond sensors. As an example, the reference signal as a function of the absorbed dose is shown in Figure 4 for two CVD diamond sensors. The size of the signal rises at small doses, a known effect called pumping, and then decreases steadily with increasing dose. The behavior of the two sensors is very similar.
The results obtained for all sensor types have been presented at IEEE conferences and will be prepared for publication[5]. The results will also be used in forthcoming discussions with the sensor producers to understand the damage mechanisms and to further improve the radiation hardness of the sensors.
A second test set-up has been built for sensor performance studies in the 3 GeV electron beam at DESY. This is a low intensity beam. A scintillator hodoscope is used as beam particle trigger. The particle trajectories are measured with the EUDET telescope comprising several planes of pixel sensors. A picture of the setup is shown in Figure 5. For the data taken the impact points of reconstructed particle trajectories in the sensor plane are calculated and distributed in Figure 6. Only beam particles with a signal in the sensor above the noise level are shown. The circular shape of the electrode on the diamond sensor is clearly seen. The data taken will be used to determine the relation between energy loss by ionisation and the amount of created free charge carriers for diamond sensors. Depending on the results, we will decide about additional test-beam campaigns.

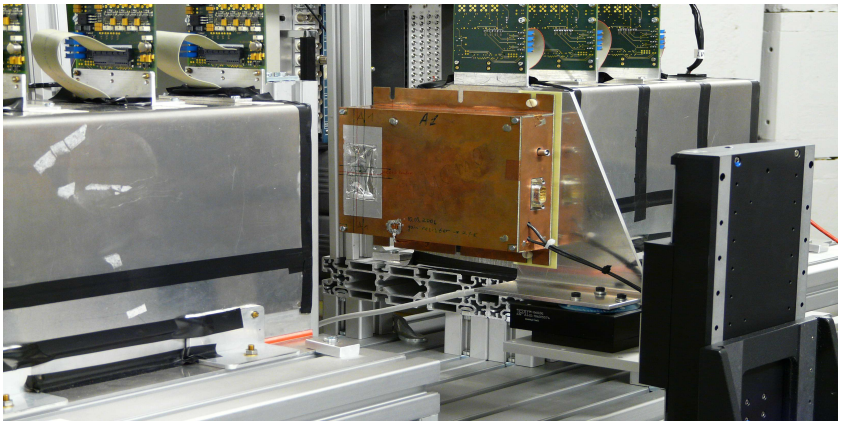

Figure 5: The test-beam setup for studies of a single crystal diamond. The sensor under test including the preamplifier is housed in the copper covered PCB box. Up- and downstream of this box the pixel sensors of the EUDET telescope are installed.

3 FE Electronics

In the current design, LumiCal consists of 30 layers of 300 μm thick DC-coupled silicon sensors [6]. Each layer is divided into azimuthal sectors and each sector is segmented into radial strips with a constant radial pitch. Such design results in pads on the sensors with capacitances between 10 pF and 100 pF.
From Monte Carlo simulations of Bhabha scattering the charge collected on the pads within an electron shower has been estimated to reach values up to 10 pC. For calibration and alignment studies, the signals from relativistic muons, i.e. minimum ionising particles, MIPs, should be detected. To resolve a MIP charges down to 2 fC have to be be measured [7].
The FE ASIC is therefore foreseen to be operated in two modes - the physics mode for measuring Bhabha electrons and the calibration mode to measure muons. Because of the high occupancy expected in the physics mode, the front-end electronics must resolve signals from particles produced in subsequent bunch crossings, i.e., in a time scale of about 300 ns. The power dissipation must be kept small to avoid large cooling pipes and thermal tensions. This should be ensured by switching off the power in the periods between the bunch trains. The requirements on the BeamCal FE ASICs are very similar.
The general concept of the FE electronics [8], matching the requirements listed, is outlined in Figure 7. The main blocks in the signal flow are: the FE ASIC, the A/D conversion ASIC and the data concentrator with the optical driver. The first block has been designed as dedicated multichannel FE ASIC and the ADC ASIC as a pipeline 10 bit ADC with 1.5-stage architecture. The prototypes are designed and fabricated using the AMS 0.35μm technology.
The results of measurements on gain, noise, high input rate performance and cross talk are reported in detail in Ref. [9]. Here a few examples will be given.

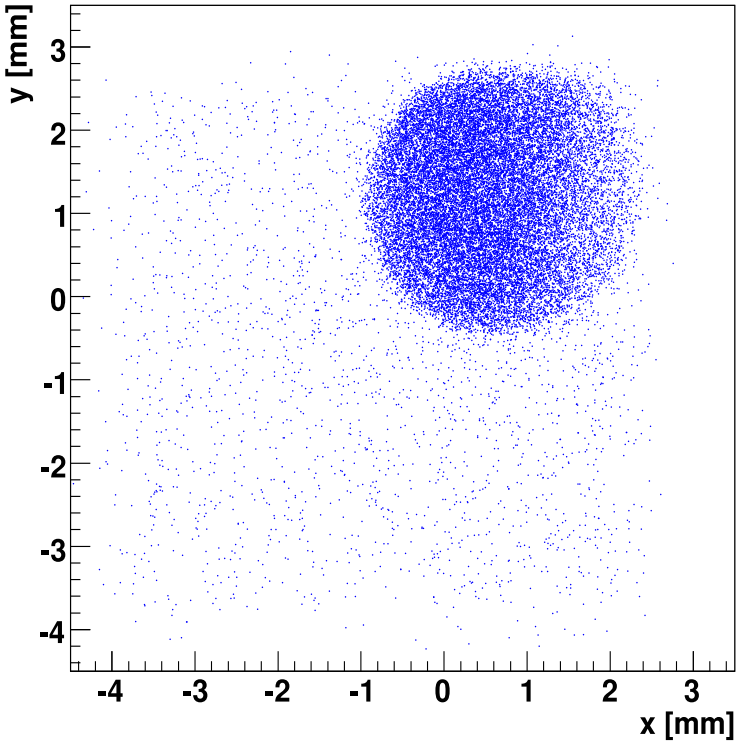

Figure 6: The distribution of the impact points of beam particles in the sensor planes when the signal in the sensor is above the noise level.

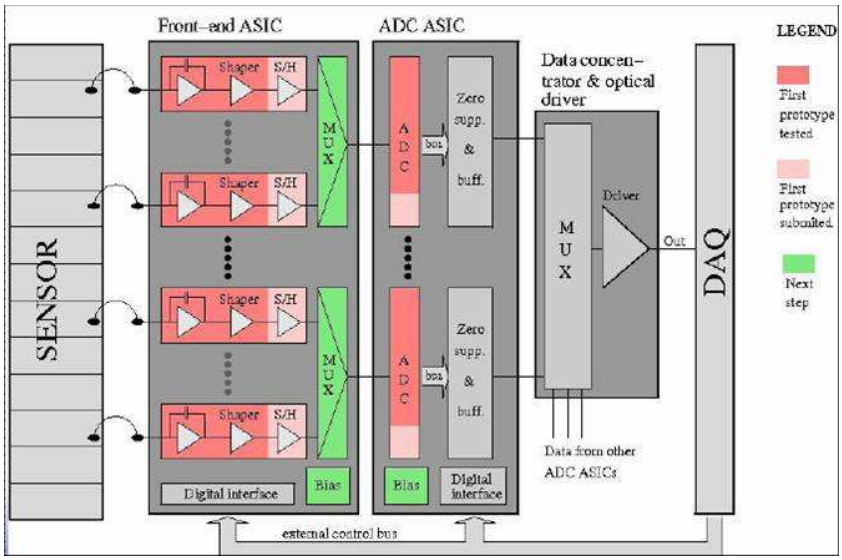

Figure 7: Block diagram of the FCAL readout electronics

3.1 Performance of FE ASIC Prototypes

An example of an FE ASIC prototype is shown in Figure 8. It comprises a charge

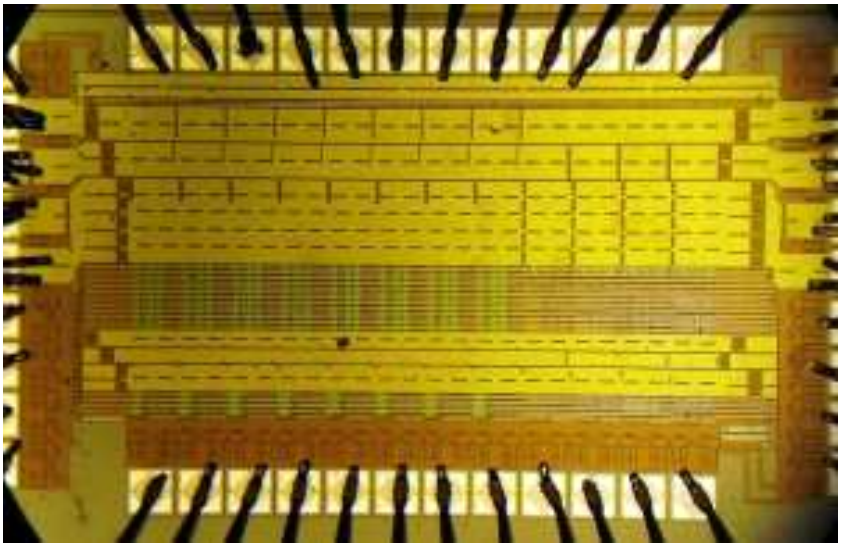

Figure 8: A prototype of the FE ASIC bonded and glued on a PCB. The first four channels from the left have passive feedback, the following four channels have a feedback using a MOS transistor.

sensitive amplifier, a pole-zero cancellation circuit and a shaper. To cope with the small charges expected for a MIP and the larger ones from an electron shower a change of the gain is implemented, to allow to switch between calibration mode and physics mode, respectively, both in the charge amplifier and the shaper. Four channels on the ASIC are operated with a feedback resistor and four channels use a MOS transistor for this purpose. The area occupied by a single channel is 630 x 100 μm^2. The ASICS are manufactured in 0.35μm four-metal, two-poly technology.
The response of the ASICs to a charge injected through the input test capacitance is shown in Figure 9 for different values of the sensor pad capacitance. In the physics mode the results for channels with a resistive feedback and the MOS feedback are the same, hence only the MOS feedback curves are shown. The amplitude and the peaking time are not sensitive to the input capacitance. In the calibration mode the amplitude and the peaking time depend slightly on the input capacitance. This dependence, more pronounced for the MOS transistor feedback, can be explained by the relatively small value of the feedback capacitance so that the ratio of the sensor pad capacitance to the effective input capacitance cannot be neglected. Measurements of the output voltage as a function of the injected charge demonstrate linearity within 2% for input charges between 1 pC and 10 pC with very small dependence on the sensor pad capacitance in the physics mode, and between 1 fC and 25 fC in the calibration mode. In the latter case a slight dependence on the sensor pad capacitance is observed, again more pronounced in the case of the MOS transistor feedback. The simulations of these parameters are in very good agreement with the measurements.

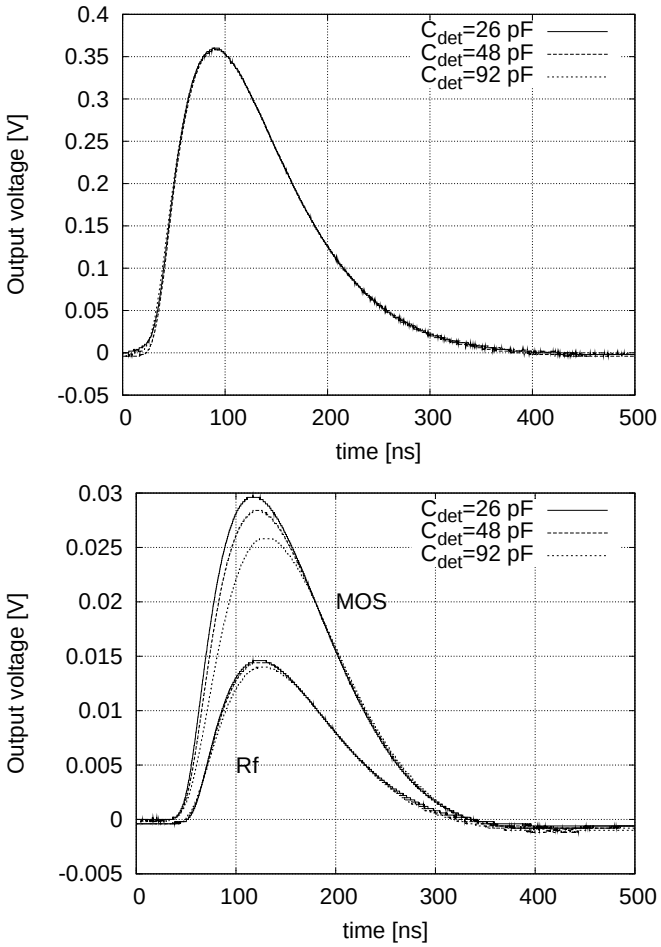

Figure 9: Output pulses for MOS transistor feedback in physics mode (top) and for MOS and resistive feedback in calibration mode (bottom) for different sensor pad capacitances.

The equivalent noise charge (ENC) measurements also confirm the simulations and match the requirements. In particular in the calibration mode the S/N is above 10 even for the largest sensor pad capacitances.
The effectiveness of the pole-zero cancellation circuit has been measured as a function of the rate of input pulses. In the physics mode the output amplitude is stable within 3% up to input signal frequencies of 3 MHz. In the calibration mode a dependence on the sensor pad capacitance is observed. Nevertheless, the change of the output amplitude is below 4% at 3 MHz. Also these measurements confirm the simulations.
Cross talk has been measured using a pin-diode flashed with a laser pulse to generate an input signal. In the calibration mode the cross talk amounts to 0.1% and 0.3% for the MOS transistor and resistive feedback, respectively. In the physics mode the measured numbers are 1% and 1.5% for the two types of feedback. These relativley large values may be explained by the very large feedback capacitor of 10 pF. This parameter will be subject of improvement in future versions of the ASIC.

The channels of one ASIC are connected to a silicon pad sensor and the signals of electrons are measured with a charge integrating external ADC. An example of a spectrum is shown in Figure 10. The signal is nicely separated from the pedestal. Being the first attempt to connect the ASIC to a sensor the result corresponds fully to our expectations.

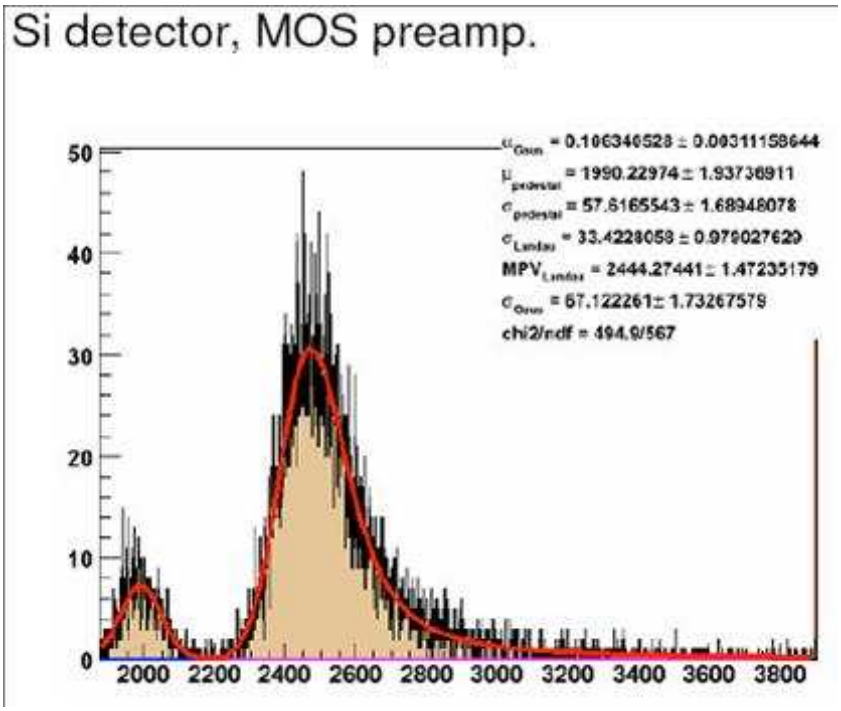

Figure 10: The signal spectrum from electrons crossing a silicon pad sensor connected to a channel of the ASIC with MOS transistor feedback.

3.2 Performance of the ADC ASICs

Prototype ASICs with 8 pipeline ADC stages have been designed and produced in 0.35 μm CMOS technology. A 1.5-bit stage architecture has been chosen because of its simplicity and immunity to offsets in the comparator and amplifier circuits. Each stage generates 2 bits which are send to a digital correction block, where the 16 output bits are combined to an 8 bit output value. An ADC ASIC prototype is shown in Figure 11. Eight additional MDAC blocks are placed around the chip. Biasing and clock generation units are located in the center of the chip. The functionality of the ADC has been tested generating input signals with a dedicated circuit based on a fast differential amplifier. For the readout a FPGA based data acquisition system connected to a PC has been used.
The integral (INL) and differential (DNL) nonlinearities have been measured statically with an ADC sampling frequency of 10 MHz to be ± 3 LSB and ± 0.5 LSB, respectively. Some codes with a larger DNL have been identified and corrected in the new version.

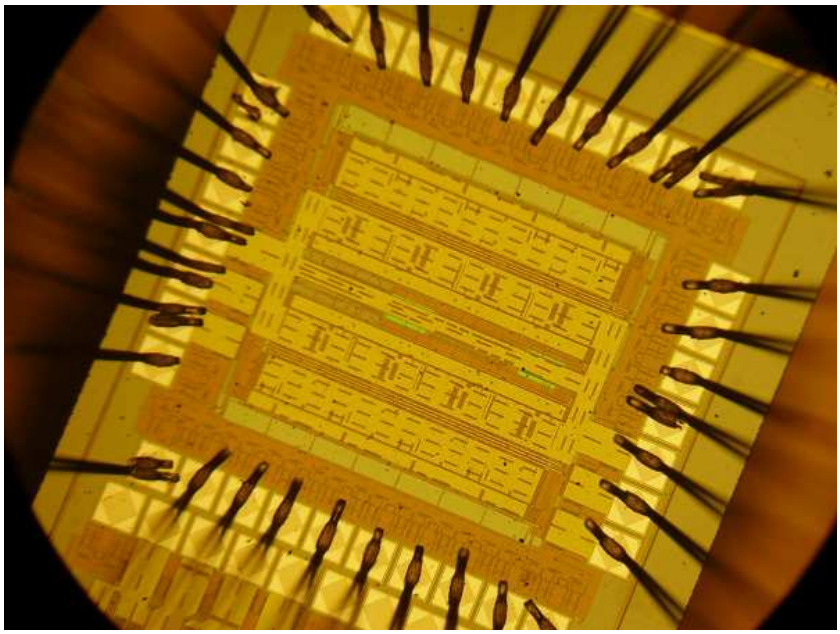

Figure 11: A prototype of the ADC ASIC glued and bonded to a PCB.

The measurement of dynamic parameters, the signal-to-non-harmonic ratio (SNHR), the spurious free dynamic range (SFDR), the harmonic distortions (THD) and the signal-to-noise and distortion ratio (SINAD) demonstrated proper functionality up to a sampling frequency of 36 MHz. The measured SNHR of 50 dB corresponds to the expected value for 8 stages. Some imperfections in the linearity are found and understood. A new prototype designed for 10 bit resolution has been already produced and is under test.

4 The Laser Position Monitoring System

A prototype of a laser based position monitoring system was built and tested in the laboratory [10]. Two narrow laser beams are directed to a CCD sensor. One beam is perpendicular to the plane of the CCD sensor and the other shines onto the sensor with an angle of 45°. Using the two laser spots on the CCD, the spot position of the perpendicular beam monitors movements in the (x-y) plane. The distance between the two spots measures the displacement in the z direction. The system, shown in Figure 12, is installed in a temperature stabilized box. The position of the CCD sensor has been controlled by using an optical linear encoder with a resolution of 0.1 μm. The laser spots on the CCD are readout, and an algorithm determines the spot centres. The resolutions obtained for displacements in the x-y plane and displacements in z-direction is 0.5 μm and 1.5 μm, respectively.
The whole setup has been placed in a temperature stabilized box and the performance of the system has been tested when the temperature was changed. The shifts in the position measurement due to temperature change have been determined to be about 1

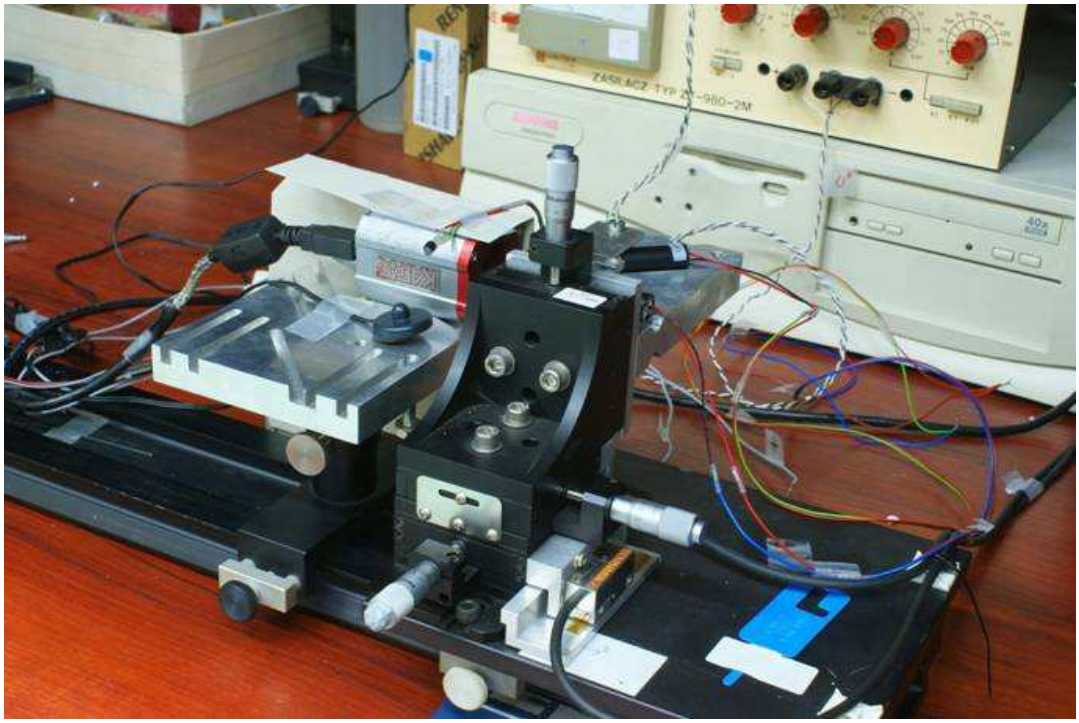

Figure 12: The prototype of the laser position displacement system. Two laser beams from diodes in rear part of the picture are recorded by an CCD sensor mounted on the precisely movable table in the foreground. For the readout of the CCD sensor a specialised FE electronics and DAQ has been developed.

μm per °C. The system was operated over several month, and monitored a reference position within 1 μm. No systematic shifts have been observed.
To apply the system at a real detector the space for the senor is extremely small. Therefore in a future version a miniature CMOS optical sensor will replace the CCD pixel sensor. For its readout a new electronics board has been developed and produced. A prototype of this board is shown in Figure 13 in the laboratory test.

5 Summary

The infrastructure for sensor tests in the laboratory has been created and upgraded at the Tel Aviv University and at DESY Zeuthen, respectively. The equipment for sensor tests in particle beams has been completed and has been used in several test-beam campaigns, e.g. together with the EUDET telescope at DESY. Prototypes of the FE readout ASICs and ADC ASICs have been produced and tested. The FE ASICs match the essential performance requirements and will be used in future test-beam studies of more complex detector components. A redesign has been done to improved the ADC ASICs. New prototypes are produced and are under test.
A prototype of the laser displacement monitor system has been built and operated over

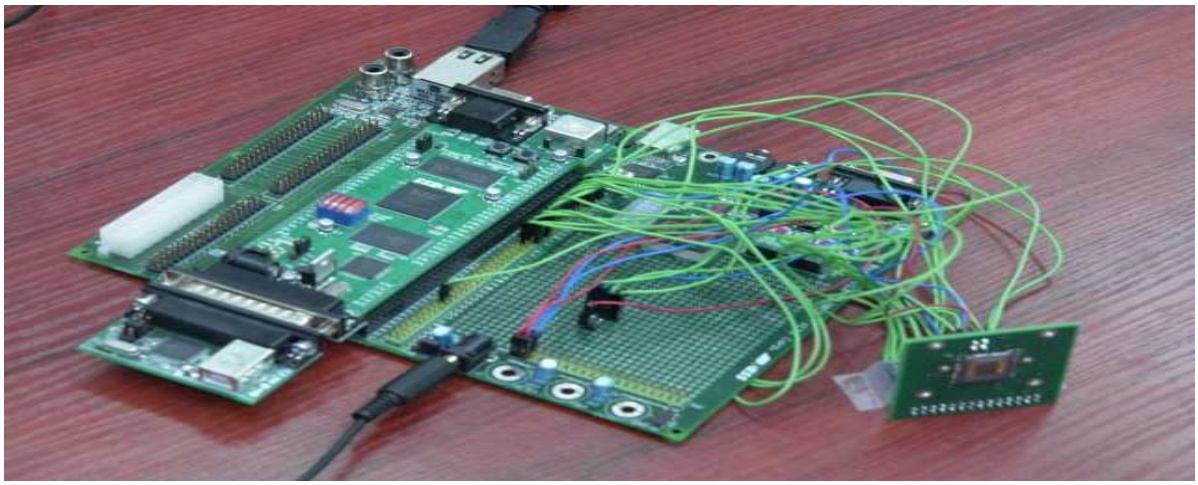

Figure 13: The readout board for the CMOS optical sensor prepared for tests

several months. It has been shown that the stability of a small-size system is on the level of 1 μm, i.e. an order of magnitude better than required.

Acknowledgment

This work is supported by the Commission of the European Communities under the 6^{th} Framework Programme "Structuring the European Research Area", contract number RII3-026126.

References

[1] H. Abramowicz et al. "Instrumentation of the very forward region of a linear collider detector", IEEE Trans. Nucl. Sci. 51:2983-2989, 2004.

[2] S. Schuwalow, "Forward Calorimetry Sensor Test Facilities", EUDET-Memo-2008-32.

[3] J. Błocki et al., "Silicon Sensors for the LumiCal", EUDET-Memo-2007-47.

[4] M. Idzik et al., "Status of VFCAL", EUDET-Memo-2008-01.

[5] Ch. Grah et al., "Polycrystalline CVD Diamonds for the Beam Calorimeter of the ILC", accepted for publication in TNS, "Radiation Hard Sensors for the Beam Calorimeter of the ILC" submitted to the Proceedings of the IEEE Conference, Hawaii, USA 2007.

[6] H. Abramowicz et al., "A Clustering Algorithm for the Luminosity Calorimeter", submitted as LC-Note, 2008.

[7] H. Abramowicz et al., "GEANT-4 Simulations of the Electronics Readout Constraints for the Luminosity Detector of the ILC", EUDET-Memo-2007-17.

[8] M. Idzik et al., "The Concept of the LumiCal Readout Electronics", EUDET-Memo-2007-13.

[9] M. Idzik et al. "Status of LumiCal Readout Electronics", EUDET-Report-2008-08.

[10] W. Daniluk et al., "Laser Alignment System for LumiCal", EUDET-Report-2008-05.